



On the utility of microfluidic systems to study protein interactions: advantages, challenges, and applications

Serena A. J. Watkin^{1,2} · Rachel Z. Bennie^{1,2}  · Jenna M. Gilkes³  · Volker M. Nock^{1,4,5}  · F. Grant Pearce^{1,2}  · Renwick C. J. Dobson^{1,2,5,6} 

Received: 11 October 2022 / Revised: 15 December 2022 / Accepted: 20 December 2022 / Published online: 30 December 2022
© European Biophysical Societies' Association 2022

Abstract

Within the complex milieu of a cell, which comprises a large number of different biomolecules, interactions are critical for function. In this post-reductionist era of biochemical research, the ‘holy grail’ for studying biomolecular interactions is to be able to characterize them in native environments. While there are a limited number of in situ experimental techniques currently available, there is a continuing need to develop new methods for the analysis of biomolecular complexes that can cope with the additional complexities introduced by native-like solutions. We think approaches that use microfluidics allow researchers to access native-like environments for studying biological problems. This review begins with a brief overview of the importance of studying biomolecular interactions and currently available methods for doing so. Basic principles of diffusion and microfluidics are introduced and this is followed by a review of previous studies that have used microfluidics to measure molecular diffusion and a discussion of the advantages and challenges of this technique.

Keywords Proteins · Protein interactions · Diffusion · Microfluidics · Laminar flow · Structural biology

Introduction: studying biomolecular interactions

Rarely in biology do molecules function in isolation; in fact, the vast majority of biological processes involve interactions between macromolecules such as proteins and nucleic acids (e.g., during transcriptional regulation (Horne et al. 2021; Wood et al. 2021), as well as lipids (e.g., by membrane transporter proteins within a cell membrane (Davies et al. 2021, 2022), as well as carbohydrates and other small molecules known as ‘ligands’ (e.g., during enzyme catalysis of carbohydrates (Currie et al. 2021). Thus, biomolecular interactions are essential for life and defining them is necessary to understand life from a molecular perspective. Knowledge of biomolecular interactions is a fundamental aspect of elucidating their function and can aid in discovering and mapping out metabolic pathways and other cellular processes. It is also important in the field of medical biochemistry for understanding disease mechanisms and developing therapeutics.

Special Issue: Analytical Ultracentrifugation 2022.

- ✉ Volker M. Nock
volker.nock@canterbury.ac.nz
- ✉ F. Grant Pearce
grant.pearce@canterbury.ac.nz
- ✉ Renwick C. J. Dobson
renwick.dobson@canterbury.ac.nz

- ¹ Biomolecular Interaction Centre, University of Canterbury, Christchurch, New Zealand
- ² School of Biological Sciences, University of Canterbury, Christchurch, New Zealand
- ³ Protein Science and Engineering Team, Callaghan Innovation, Christchurch, New Zealand
- ⁴ Department of Electrical and Computer Engineering, University of Canterbury, Christchurch, New Zealand
- ⁵ The MacDiarmid Institute for Advanced Materials and Nanotechnology, Wellington, New Zealand
- ⁶ Department of Biochemistry and Molecular Biology, Bio21 Molecular Science and Biotechnology Institute, University of Melbourne, Melbourne, VIC, Australia

Existing techniques: a brief review

Given the importance of characterizing biomolecular interactions, a wide variety of experimental approaches have been developed to analyze them. While some techniques are aimed simply at detecting an interaction, others are capable of identifying interfaces involved or determining binding affinities and kinetics of the interaction. A brief summary of the (dis)advantages of these approaches is shown in Table 1.

Some methods rely on the proximity of interacting molecules producing a signal, such as *in vivo* expression of a protein or change in fluorescence emission. For example, two-hybrid screening (also known as yeast 2-hybrid or Y2H) entails detecting protein–protein interactions by splitting the activating and binding domains of a transcription factor and hybridizing each domain with one of the two potential interacting proteins, such that transcription of a reporter gene can only be activated when the two hybrid proteins interact (Brückner et al. 2009). One-hybrid screening can also be used to detect protein–DNA interactions (Ouwkerk and Meijer 2001), while three-hybrid systems can be used to detect protein–RNA interactions (SenGupta et al. 1996). Protein complementation assays work on a similar principle, but rather than using a transcription factor *in vivo*, a reporter protein that can produce a signal independently, such as

firefly luciferase (either *in vivo* or *in vitro*), which overcomes certain drawbacks of the Y2H method (Ratray and Foster 2019). Molecular proximity can also be detected (*in vivo* or *in vitro*) by Förster resonance energy transfer (FRET) between fluorophores fused to interacting proteins (Royer and Scarlata 2008); for example, between cyan and yellow fluorescent proteins (Dinant et al. 2008). These techniques generally only detect an interaction between two partners and do not provide any details of the interaction. Perhaps the key advantage, however, is that they can be performed within a cell milieu, which best mimics the native-like environments where the interactions occur.

Several *in vitro* experimental approaches to detecting biomolecular interactions rely on detecting changes on a surface on which a target biomolecule is immobilized when exposed to potential interacting molecules. For example, the quartz crystal microbalance (QCM) detects interactions by changes in mass on the surface of a quartz crystal via changes in its resonant frequency (Cheng et al. 2011). Biomolecular interactions can also cause a change in optical properties of the surface, such as refractive index or interference of reflected light, which is the basis for surface plasmon resonance (SPR) (Wilson 2002) and bio-layer interferometry (BLI) (Concepcion et al. 2009; Shah and Duncan 2014), respectively. In general, these techniques can only be performed in ideal buffered conditions, although they will afford highly

Table 1 Summary of advantages and disadvantages to approaches that detect biomolecular interactions

Type	Technique	Advantages	Disadvantages
Proximity	Yeast-2-hybrid	Performed in native cell environment	Does not provide binding constants
	FRET	Can be performed in native cell environment	Requires labeled protein
Surface immobilization	Quartz crystal microbalance (QCM)	Provides detailed binding constants	Requires immobilization of protein
	Surface plasmon resonance (SPR)	Provides detailed binding constants	Requires immobilization of protein
	Bio-layer interferometry (BLI)	(1) Provides detailed binding constants (2) Can use crude lysates	Requires immobilization of protein
Co-migration–matrix	Native PAGE	Does not require specialist equipment	(1) Does not provide binding constants (2) Matrix may perturb interactions
	Size exclusion chromatography	Does not require specialist equipment	Matrix may perturb interactions
	Electrophoretic mobility shift assay (EMSA)	Does not require specialist equipment	Matrix may perturb interactions
Co-migration–matrix free	Field-flow fractionation (FFA)	No interaction with surfaces or matrix	Requires high protein concentrations
	Analytical ultracentrifugation (AUC)	(1) Provides detailed binding constants (2) Can use crude lysates	
Heat based	Microscale thermophoresis (MST)	Provides detailed binding constants	Requires highly pure samples
	Isothermal titration calorimetry (ITC)	Provides detailed binding constants	Requires highly pure samples
Spectroscopy	Nuclear magnetic resonance (NMR)	(1) Provides detailed binding constants (2) Can use crude lysates	Requires labeled protein

detailed information about the interaction; for example, SPR will allow the determination of the k_{on} and k_{off} rates.

Other techniques that require immobilization of binding partners include co-immunoprecipitation (Co-IP), which uses antibodies bound to the surface of agarose or magnetic beads onto which the target protein (antigen), along with any interacting proteins are precipitated. While Co-IP is used to detect protein–protein interactions, chromatin immunoprecipitation (ChIP) can similarly be used to detect protein–DNA interactions (Collas 2010) and ribonucleo-protein immunoprecipitation (RIP) (Keene et al. 2006) is used for protein–RNA interactions. Pull-down assays also use a protein immobilized to a bead, but in this case the target protein is tagged (e.g., with GST, biotin) and captured by beads with the corresponding affinity ligand (e.g., glutathione, streptavidin) using affinity chromatography. These techniques work well for identifying protein binding partners in native-like cell lysates, but have the disadvantage of non-specific binding and requiring an extrinsic tag. Phage display (Smith and Petrenko 1997) is a high-throughput method for screening protein–protein or protein–DNA interactions which involves immobilization of target molecules on the surface of a microtiter plate well. Rather than screening a cell lysate for interacting partners, a library of phages displaying proteins of interest inserted into phage coat proteins is used, with those that display interacting partners binding to the surface while others are washed away.

Co-migration techniques do not require immobilization, but instead depend on interacting molecules migrating together while being fractionated and subsequently identified by another method (e.g., mass spectrometry or western blot). Fractionation can be carried out by chromatography (e.g., size exclusion, ion exchange) or electrophoresis (e.g., native polyacrylamide or agarose gel) (Ratray and Foster 2019). Electrophoretic mobility shift assays (EMSA) are a specific example of this technique, commonly used to detect protein–DNA interactions by observing differences in the migration of DNA in the presence and absence of protein (Hellman and Fried 2007).

Field-flow fractionation (FFF) also works on the principle of interacting species co-migrating in solution; however, it does not utilize a matrix such as a gel or chromatography column, but rather a force field (e.g., electric, magnetic, gravitational etc.) operating perpendicular to the direction of fluid flow along a channel to fractionate different sized molecules (Chou et al. 2011). This separation method is gentler and therefore better at detecting weaker interactions compared to the aforementioned techniques where the matrix may perturb interactions (Chou et al. 2011). Analytical ultracentrifugation (AUC) is also matrix free and uses a centrifugal force field to separate components based on their size, although in this case they are only temporarily separated and are detected while still in the force field, rather

than being eluted into different fractions for detection at the end (Uchiyama et al. 2016). Thus, AUC requires some prior knowledge of the composition of the sample to identify new interactions. The addition of a fluorescence detection system to AUC has extended its capabilities, allowing analysis of protein–protein interactions with dissociation constants (K_D) in the nanomolar and even picomolar range and of highly concentrated solutions (MacGregor et al. 2004; Kingsbury and Laue 2011; Zhao et al. 2013, 2014; Chaturvedi et al. 2017). Additionally, AUC with fluorescence detection allows for detection of sedimentation in native-like complex environments, such as serum (Demeule et al. 2009; Kingsbury et al. 2012; Hill and Laue 2015; Krayukhina et al. 2017; Wright et al. 2018b; Mehn et al. 2020), or cell lysates (Kroe and Laue 2009).

Heat-based approaches include microscale thermophoresis (MST), which measures movement of molecules along a local temperature gradient using an infrared laser and fluorescence detection (Seidel et al. 2013), and isothermal titration calorimetry (ITC), which measures small changes in heat in solution to detect and measure the binding affinity of an interaction (Ladbury and Chowdhry 1996). ITC is typically used to analyze protein–ligand interactions, but has also been used to characterize protein–protein interactions. Although these are able to provide unique information on the interaction (e.g., ITC provides both the ΔH and ΔS of interaction along with the K_D), again they are generally only conducted in carefully buffered conditions that are far from the native conditions of the cell.

Spectroscopic techniques such as NMR can be used to measure protein–protein interactions through chemical shift perturbation analysis, in which spectra of a labeled protein is collected in a series of varying concentrations of unlabeled ligand (Purslow et al. 2020). An advantage of this technique is that it can also provide structural information about the nature of binding. The use of in-cell NMR can allow the study of biomolecules within living cells, allowing for the study of proteins in the native environment (Barbieri et al. 2015; Li et al. 2017).

Theory of diffusion

Some methods for analyzing biomolecular interactions depend on measuring diffusion, and so basic principles of molecular diffusion are introduced here. Since this review is intended as a starting point for those new to the field, many of the references below are themselves reviews or text books that nicely introduce the topics in more depth than here and the reader can also find with these the primary literature, which at times is not so accessible.

Diffusion is the spontaneous process that, in the presence of a concentration gradient, causes molecules to move from regions of high concentration to low concentration. It results in the mixing of molecules by random movements, driven by their thermal motion, and without bulk fluid flow (i.e., in the absence of advection). The process of diffusion in gases, liquids and solids has been studied for almost two centuries, with physical concepts and mathematical descriptions being contributed by many scientists, including Fick (Philibert 2006) and Einstein (Einstein 1956) who considered the process from macroscopic and microscopic points of view, respectively.

Fick's laws: diffusion from a macroscopic perspective

Fick's first law for diffusion in one dimension states that the diffusive flux (F) is proportional to concentration gradient ($\partial c/\partial x$) in this dimension (Crank 1975):

$$F = -D \left(\frac{\partial c}{\partial x} \right). \quad (1)$$

The proportionality constant D is the diffusion coefficient (also referred to as 'diffusivity'), which has units of length squared per unit time. The diffusion coefficient depends on the physicochemical properties of the diffusing molecules (size, shape), and on properties of the medium through which it diffuses (viscosity, temperature) (Linder et al. 1976).

Applying the law of conservation of mass yields Fick's second law, which describes how the diffusion of sample molecules causes the concentration gradient to change with time (Crank 1975; Linder et al. 1976):

$$\frac{\partial c}{\partial t} = \frac{\partial}{\partial x} \left(D \frac{\partial c}{\partial x} \right). \quad (2)$$

With the assumption that the diffusion coefficient is independent of concentration (Crank 1975; Linder et al. 1976), and hence independent of x -position, Fick's second law reduces to:

$$\frac{\partial c}{\partial t} = D \frac{\partial^2 c}{\partial x^2}. \quad (3)$$

This assumption is only valid for dilute solutions of biomolecules, due to thermodynamic non-ideality (Creighton 2010).

The Einstein equation: diffusion from a microscopic point of view

Whereas Fick's laws describe diffusion from a macroscopic perspective in that they consider concentration changes in a system, Einstein considered diffusion from the point of view

of individual molecules that make up fluids. The Einstein equation relates the translational diffusion coefficient to the mean square displacement $\langle R^2 \rangle$ of a collection of particles over time, based on their random thermal motion in three dimensions, and in the absence of a concentration gradient (Philibert 2006; Creighton 2010):

$$D = \frac{\langle R^2 \rangle}{6t}. \quad (4)$$

Although D is dependent on the temperature and viscosity of the solution through which the particle is diffusing, small globular proteins (from ~10 to 150 kDa) have a normalized diffusional coefficients ($D_{20,w}^0$) of ~5–12 $\times 10^{-7}$ cm²/s, which means that they will diffuse (in pure water at 20 °C) roughly 12–30 μ m in 1 s (Creighton 2010).

Relating the diffusion coefficient to molecular properties

Since the same diffusion coefficient characterizes the thermal motion of molecules in the absence of a concentration gradient as that described by Fick's laws, it can be measured in a macroscopic sense, by monitoring concentration gradients over time, and related back to properties of microscopic molecules. The diffusion coefficient is a useful quantity to measure, since the rate at which a molecule moves through solution provides information about its size, shape and molecular mass (Creighton 2010). Small, spherical molecules move faster, and thus have a higher diffusion coefficient relative to large, asymmetrical molecules (Creighton 2010). The Stokes–Einstein equation illustrates the dependence of the diffusion coefficient on the size of a molecule, as well as temperature, T and viscosity, η (Creighton 2010):

$$D = \frac{k_B T}{6\pi\eta r_H}, \quad (5)$$

where k_B is the Boltzmann constant. The quantity $6\pi\eta r_H$ describes the frictional coefficient, f , of a perfect sphere with a hydrodynamic radius r_H (also known as the Stokes radius). The hydrodynamic radius of a non-spherical particle is defined as the radius of the sphere that would have the equivalent diffusion coefficient (Hatch et al. 2004; Creighton 2010). It should be noted that the Stokes–Einstein equation is based on large spheres in an infinite volume of fluid and breaks down with small molecules, when Van der Waals forces become relevant (Li 2009). Diffusion transitions from molecular behavior described by the fractional Stokes–Einstein relationship to particle behavior described by the classical Stokes–Einstein relationship in the 150–300 nm diameter range, depending on concentration (Coglitore et al. 2017).

While diffusion coefficients give a good indication of the size of molecules, accurate estimates of molecular mass from diffusion coefficients, just as for sedimentation coefficients determined by analytical ultracentrifugation, require knowledge of the shape and hydration of the molecule (Creighton 2010). However, for a series of molecules of similar shape and hydration, a power-law relationship exists, with the shape of the molecule determining the exponent (Creighton 2010):

$$D = KM^{-\varepsilon}, \quad (6)$$

where K is a constant. For spherical molecules, $\varepsilon = 0.33$ (Creighton 2010); thus, D is approximately proportional to the inverse cubed root of molecular mass (Hatch et al. 2004). For a rod $\varepsilon = 0.85$ and for a random coiled polymer $\varepsilon = 0.5 - 0.6$ (Creighton 2010).

Established methods for determining diffusion coefficients include: dynamic light scattering (DLS) (Solovyova et al. 2001; Creighton 2010; Saluja et al. 2010; Arosio et al. 2016), fluorescence correlation spectroscopy (FCS) (Creighton 2010; Sengupta et al. 2014), analytical ultracentrifugation (Squire et al. 1968; Stafford and Szent-Gyorgyi 1978; Philip et al. 1979; Cole et al. 2008; Creighton 2010; Uchiyama et al. 2016; Wright et al. 2018a), and pulsed-field gradient nuclear magnetic resonance (PFG-NMR) (Lin and Larive 1995; Bon et al. 1999; Germann et al. 2007; Creighton 2010). However, recent work by Yates et al. (2015) suggests that microfluidic techniques are equally well suited for determining diffusion coefficients.

Principles of microfluidics

The interdisciplinary field of microfluidics encompasses the science and technology underlying the development of devices that manipulate small volumes of fluids within micron-scale channels. Microfluidic chips can be designed with interconnected networks of channels and chambers to integrate a range of functions on a single, miniature device, often referred to as a ‘lab-on-a-chip’ (LoC) or ‘micro total analysis system’ (μ -TAS). The modular capabilities of microfluidic technology afford a great deal of experimental versatility for sample preparation; for instance, mixing, buffer exchange or fluorescent-labeling modules upstream of the measurement module, can all be incorporated in a single device.

Fluid theory

The relative importance of various physical phenomena changes dramatically as fluid compartments are reduced to the microscale (Squires and Quake 2005); thus, fluids behave quite differently in microfluidic channels compared to in the

macroscopic world (Weigl and Yager 1997). There are several dimensionless numbers that express the ratio of competing physical phenomena operating in fluidic systems (Squires and Quake 2005), two of which are particularly relevant to this work, and will be described here.

The first relevant dimensionless number is the Reynolds number (Re), which describes the ratio of inertial to viscous forces (Weigl et al. 1996; Brody et al. 1997; Weigl and Yager 1997, 1999; Squires and Quake 2005):

$$Re = \frac{\rho v L}{\eta}, \quad (7)$$

where ρ is the fluid density, v is the flow velocity, L is the characteristic dimension of the channel, and η is the fluid viscosity. For small channel dimensions, the Reynolds number is low, meaning that viscous forces dominate, and so an aqueous solution behaves more like a viscous oil (Squires and Quake 2005). In low Reynolds number systems, fluid flow is typically ‘laminar’, which means it occurs in smooth parallel streams, with no significant mixing between streams other than by diffusion (Weigl et al. 1996). A $Re < 1$ corresponds to pure laminar flow, while a $Re > 1000$ is approaching turbulent flow (Brody et al. 1996).

The second dimensionless number of relevance to this work is the Péclet number (Pe), which describes the ratio of the advective transport rate to the diffusive transport rate (Squires and Quake 2005) and can be expressed as:

$$Pe = \frac{vw}{D}, \quad (8)$$

where v is the flow velocity, w is the width of the channel and D is the diffusion coefficient. The Péclet number defined here provides an indication of the distance along the channel (in terms of channel widths), and hence the time required for complete mixing of two adjacent flow streams by considering both advection and diffusion (Squires and Quake 2005). As microfluidic devices generally operate in the presence of flow, advective transport does occur in the direction of flow; however, in the absence of turbulence, the low Reynolds number means that transport perpendicular to the flow direction is governed solely by diffusion (Yager 2003). The scale of the Pe number encountered depends on the channel width (200–400 μm), flow velocity in channel (50–300 $\mu\text{L/h}$) and diffusivities (from 27 $\mu\text{m}^2/\text{s}$ for Thyroglobulin to 107 $\mu\text{m}^2/\text{s}$ for Ribonuclease A). A combination of these values yields Pe numbers from ~ 1300 (for Ribonuclease A at 50 $\mu\text{L/h}$ in 100 μm deep channels) to $\sim 64,000$ (for Thyroglobulin at 300 $\mu\text{L/h}$ in 50 μm deep channels).

Fluid control

A steady, controlled flow rate is crucial for the microfluidic systems. Generating and controlling fluid motion in microfluidic devices has been achieved in several ways, including by pressure-driven and electroosmotic flow (Kamholz et al. 2001). Electroosmotic flow has the advantage of generating a velocity profile that is nearly uniform across the channel width, in contrast to pressure-driven flow, in which the velocity profile is parabolic (Kamholz et al. 2001). However, pressure-driven flow can be achieved by a simple positive-displacement syringe pump and is unaffected by ionic strength and pH of solutions, and thus is often the method of choice (Kamholz and Yager 2001; Kamholz et al. 2001).

Microfluidics for measuring molecular diffusion

Microfluidics is well suited to making measurements of diffusion, due to the low Reynolds number and intermediate Péclet number conditions operating in microchannels (described above), which together dictate that the transport of molecules perpendicular to the flow direction relies entirely on diffusion and that mixing occurs on a timescale suitable for measurements (Weigl and Yager 1997). This has been demonstrated, firstly by the Yager group, who developed a microfluidic device which they named the ‘T-sensor’ and used it to measure the diffusion coefficients of several molecules (ranging in size from ~800 to ~66 kDa) including biotin, insulin, streptavidin and human serum albumin (HSA) (Kamholz et al. 1999, 2001). More recently, the Knowles group measured the hydrodynamic radius (r_H) of various proteins using a similar diffusion-based microfluidic technique, demonstrating that proteins of differing secondary and tertiary structure, as well as intrinsically disordered proteins, and those that exist as monomeric species or as complexes can all be accurately sized by this method (Yates et al. 2015). Further, they have shown that the average r_H obtained from a mixture of monomeric and dimeric bovine insulin hormone corresponds to the ratio of each species present, indicating the tolerance of the technique for heterogeneous mixtures (Yates et al. 2015).

Measurement principle

While there are a few different microfluidic approaches to measuring diffusion (Hatch et al. 2001; Li 2009; Dey et al. 2014; Yates et al. 2015; Arosio et al. 2016), each with their own advantages and limitations for certain applications, those discussed here all rely on the same basic principle: when two (or more) fluid streams come into contact in a laminar flow device, with one containing sample molecules

and the auxiliary stream containing only solvent, the concentration gradient across the channel generates a diffusion potential perpendicular to the direction of the flow, which causes sample molecules to be transported into the auxiliary solvent stream(s) (Hatch et al. 2001, 2004; Yates et al. 2015) (Fig. 1). Diffusion coefficients can be determined by measuring the diffusion distance across the channel width after a known residence time (Yates et al. 2015), which is controlled by the flow velocity and traversed length of the channel (Hatch et al. 2001). The technique has most commonly involved only two input streams, but three input streams has been demonstrated (Weigl et al. 1999; Sengupta et al. 2014), and with two or more outlets, it becomes a molecular separation method similar to field-flow fractionation (Weigl and Yager 1999; Yager 2003; Sengupta et al. 2014; Yates et al. 2015).

Detection methods

As path lengths in microfluidic devices are inherently small, the sensitivity of traditional optical detection methods is limited (Weigl and Yager 1999; Costin and Synovec 2002). Fluorescence emission has been the most commonly detected optical signal in the microfluidic systems discussed here (Kamholz et al. 1999; Li 2009; Sengupta et al. 2013; Yates et al. 2015). Previously, absorbance has generally only been feasible for highly absorbing species (Costin and Synovec 2002) but more recently 2D UV/Vis detection platforms have been developed for on-chip absorbance measurements. For example, with the ActiPix™ D100 UV area imaging system (Paraytec), (Yates et al. 2015) determined the minimum detectable concentration of BSA is 1.25 μM using a cyclic olefin copolymer chip with a thickness of 1.7 mm and sample pathlength 320 μm .

The main drawback of fluorescence detection is the requirement for a fluorescent analyte, which typically necessitates chemical modification of the sample to incorporate an extrinsic fluorescent label. However, this limitation can be overcome if a chip with a split outlet is used, by determining the concentration of unlabeled sample molecules in each output solution as a measure of how far across the channel they have diffused (Yager 2003). In this way, the measurement and detection steps are decoupled, and thus samples are unlabeled when their diffusivity is probed (Yates et al. 2015). Knowles et al. used this ‘latent’ approach, as they refer to it, and incorporated a fluorescent-labeling module into their device for immediate subsequent concentration determination on-chip. In that setup, molecules that have diffused a certain fraction of the channel width at the end of the measurement module are diverted to the labeling module, and subsequently detected (Yates et al. 2015).

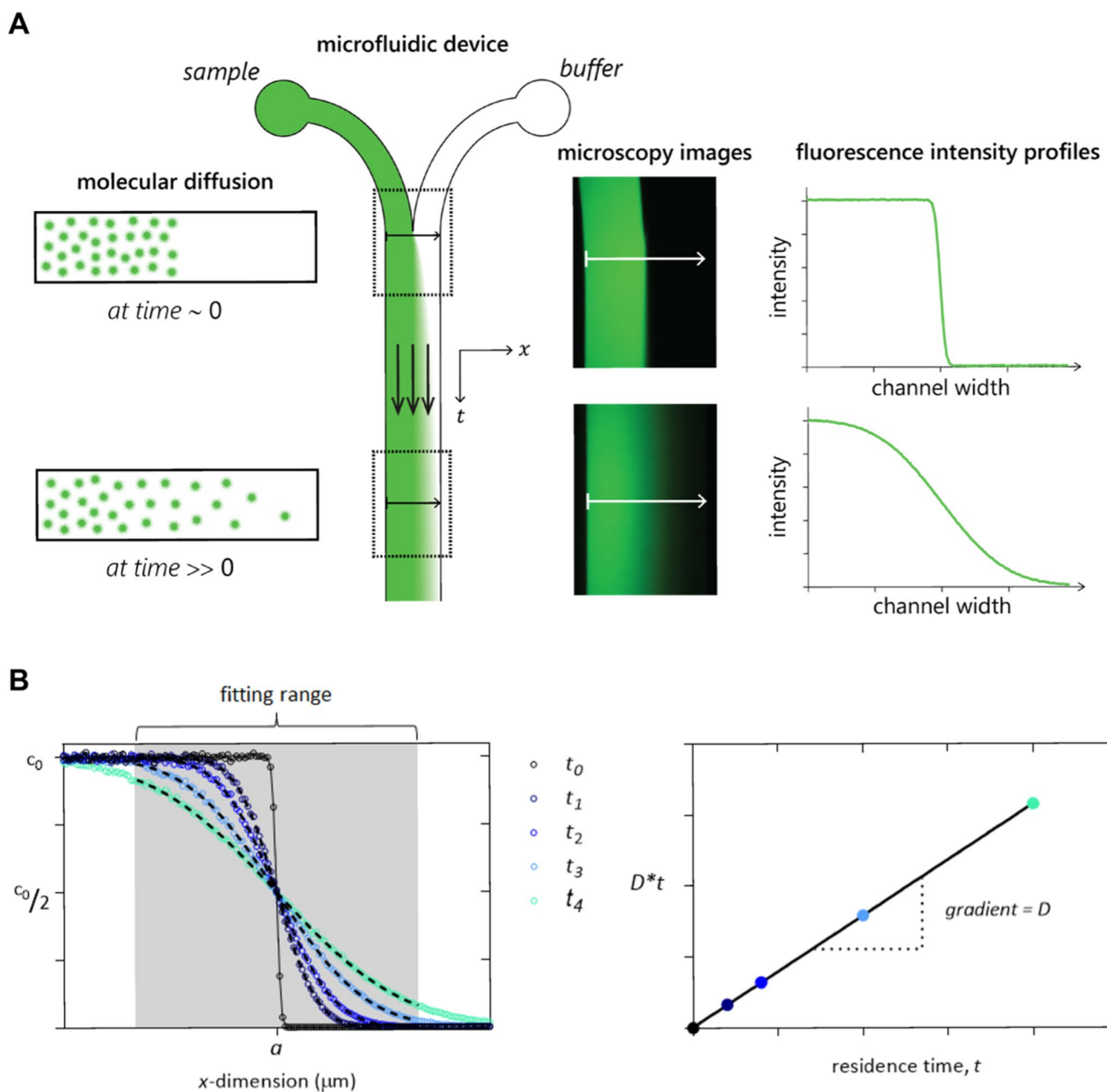


Fig. 1 **A** When a fluid containing sample molecules is brought into contact with a buffer fluid in a microfluidic laminar flow device, the resulting concentration gradient across the channel width generates a diffusion potential orthogonal to the direction of the flow, which causes sample molecule to be transported into the buffer stream. Continuous flow at a constant flow rate converts the distance along the channel length to a time coordinate, resulting in a steady-state system. Fluorescence microscopy images acquired at different time points capture the rate at which the con-

centration gradient is abolished by diffusion and this can be used to calculate the diffusion coefficient of the diffusing molecule, which is a measure of its size. **B** Determining the diffusion coefficient from fluorescence intensity profiles. Non-linear fitting of simulated fluorescence intensity profiles within a defined fitting range (gray). When the diffusion coefficient and residence time are combined and globally fitted as a single parameter (D^*t), plotting this against time yields the diffusion coefficient from the gradient

Advantages

There are several advantages of this technique; some generally applicable to microfluidics, such as short processing times, low sample consumption and hence, low cost, along

with the potential for integration with other microfluidic modules (Hatch et al. 2004). More specifically, as a sizing technique, this method has the advantage of being carried out in solution, in the absence of matrices or applied fields, and without the need for immobilization (Kamholz et al.

1999; Yates et al. 2015; Arosio et al. 2016). The combination of continuous-flow and the steady-state nature of this microfluidic system, means that multiple images can be integrated over time to increase sensitivity, without a time limit imposed by photobleaching in the case of fluorescence detection, or the rate of sedimentation, in contrast to alternative methods such as analytical centrifugation (Weigl and Yager 1999; Kamholz et al. 2001). Furthermore, since large particles such as blood cells do not diffuse significantly in typical measurement timescales, this technique is tolerant of complex solutions such as blood (Weigl and Yager 1997; Kamholz et al. 1999, 2001; Weigl et al. 1999; Hatch et al. 2004). The selectivity of fluorescence detection also enables only the molecule of interest to be detected, which is also desirable for measurements in complex solutions.

Technical challenges

The main complications with this microfluidic method for measuring diffusivity arise primarily as a result of the shape of the flow velocity profile of pressure-driven laminar flow in microchannels. Due to the ‘no-slip’ boundary condition, the velocity must be zero at the walls, which produces a parabolic velocity profile and this has several effects on the analysis, as described below.

Entrance effects

The first complication concerns the distance required to reach a fully developed velocity profile, termed the entry length. Since the velocity profile in each inlet channel will be parabolic, the velocity at the midpoint of the central channel in which the two streams merge will initially be zero, and accelerate to the final velocity (Kamholz et al. 2001; Yager 2003). Therefore, knowledge of the entry length is needed to inform the data collection strategy, ensuring that measurements are made downstream of this channel distance (Kamholz et al. 2001; Yager 2003). This can also lead to over-prediction of diffusion coefficients if the entry length is not accounted for when calculating the time that the molecules have spent in the channel (Kamholz et al. 2001). (Kamholz et al. 2001) quantified these entrance effects using hydrodynamic simulations and found that the entry length is independent of flow rate in the range they studied.

The butterfly effect

A second problem related to the velocity profile has been referred to as the “butterfly effect” (Kamholz et al. 1999, 2001; Kamholz and Yager 2001, 2002; Yager 2003) as it results in a butterfly or hourglass shape in the cross section of the interdiffusion zone, as visualized by fluid dynamic simulations (Kamholz et al. 1999; Kamholz and

Yager 2001) and by confocal microscopy (Ismagilov et al. 2000). Since the distance a molecule diffuses depends on the time it spends in the channel, which in turn depends on the flow velocity, molecules situated near the top and bottom walls of the channel where the flow velocity is slower will diffuse further compared to those in the center of the channel (Ismagilov et al. 2000; Kamholz and Yager 2001, 2002; Yager 2003; Sengupta et al. 2013). Ismagilov et al. (Ismagilov et al. 2000) showed that, rather than following the one-half power scaling law described by the Einstein equation, the diffusion distance in regions near the top and bottom channel walls scales as the one-third power (Ismagilov et al. 2000). This introduces a concentration gradient in the vertical dimension of the channel, which causes diffusion to occur in a second dimension, and thus the one-dimensional models of diffusion can no longer be accurately applied (Kamholz and Yager 2001, 2002). However, at greater distances into the channel, the butterfly effect diminishes, as the concentration gradient is abolished by diffusion in the vertical dimension of the channel. Thus, at sufficient downstream distances, the butterfly effect becomes negligible and one-dimensional models with one-half power scaling laws can be used throughout the channel height (Kamholz and Yager 2002). Since this difference in scaling laws is dependent on the relative time scales of fluid advection and diffusion, the Péclet number (Eq. 8) can be used as an indicator of this phenomenon (Kamholz and Yager 2001). The aspect ratio (width/height) of the channel is a critical factor in governing the influence of this effect on measurements, as the equilibration time in the vertical dimension will be lengthened proportionally to the square of the channel height (Weigl et al. 1996). A high aspect ratio is also important for maximizing the uniformity of the velocity profile across the horizontal dimension of rectangular channels, which is desirable in these systems, to avoid the complication of calculating position-dependent residence times (Weigl et al. 1996; Kamholz et al. 1999, 2001; Kamholz and Yager 2001; Yager 2003). For an aspect ratio > 20, Yager et al. determined the velocity profile to be uniform for at least 90% of the channel width (Kamholz and Yager 2001).

Viscosity effects

While this diffusion-based microfluidic technique is generally more tolerant than other techniques to complex biological samples, such as blood, the viscosity of the sample relative to the buffer can significantly affect the performance of these devices (Kamholz et al. 1999; Yager 2003; Hatch et al. 2004). A sample with a higher viscosity relative to the buffer will occupy a larger proportion of the channel and move through it with a lower average velocity, forcing the buffer stream to move with a higher velocity (Kamholz et al. 1999; Yager 2003; Hatch et al. 2004). The shift in the

fluid interface from the channel midpoint can complicate the analysis (depending on the method used) (Hatch et al. 2004), and moreover, the difference in velocity between the two fluid streams has the potential to interfere with the diffusion process (Hatch et al. 2004). Given that the diffusion coefficient depends on solution viscosity (Eq. 5), local viscosity changes as a consequence of diffusing molecules, which cannot easily be accounted for, is also potentially problematic for diffusivity measurements (Kamholz et al. 1999; Hatch et al. 2004).

In contrast to the butterfly effect, the sample viscosity effect described above is more pronounced in channels with higher aspect ratios (Hatch et al. 2004). Therefore, an aspect ratio must be chosen such that an acceptable compromise between these two unfavorable effects is achieved.

Summary and applications

Analytical tool

In addition to measuring simple diffusion coefficients, the earliest work in this field by Yager et al. was aimed at developing their T-sensor as an analytical tool for measuring the concentration of a molecule of interest or the kinetics of a reaction (Kamholz et al. 1999; Hatch et al. 2004). While still taking advantage of diffusion potentials in laminar flow devices, this technique relies on the interdiffusion of reacting species producing a signal, such as a color change of an indicator, rather than measuring a change in diffusive transport (Kamholz et al. 1999; Hatch et al. 2004). The first demonstration of this was the measurement of H^+ ion concentration (pH), initially in buffer (Weigl et al. 1996), and subsequently in whole blood (Weigl et al. 1999). As another example, the molecule AB580, which produces a fluorescent signal upon binding HSA, was used to determine HSA concentration and it was also shown how binding equilibrium constants and on/off rates could be derived from fitting experimental data to an appropriate analytical model (Kamholz et al. 1999). A ‘premixed’ diffusion-based assay was later proposed for interaction systems with low binding rates, in which binding partners (in this case, fluorescein and bovine serum albumin) were premixed and allowed to reach equilibrium before being introduced into the T-sensor (Hatch et al. 2004).

Immunoassay

As an extension of their earlier work using the T-sensor, the Yager group developed a diffusion-based immunoassay that was able to measure the concentration of an anti-epileptic drug molecule, phenytoin, at clinically relevant levels in diluted whole blood (Hatch et al. 2001). Based on the principle that the diffusivity of a small molecule antigen changes

upon binding a large molecule antibody, it is postulated that concentrations of the antigen, or the affinity of the analyte for its binding partner can be measured (Hatch et al. 2001). In a ‘competitive’ immunoassay format, the concentration or binding affinity of an unlabeled antigen can be probed by measuring the diffusivity of a labeled antigen which competes for the antibody binding sites (Hatch et al. 2001). In this way, the molecule of interest does not have to be directly observable as it is the diffusivity of an indicator molecule which is measured (Hatch et al. 2004). Dilution of blood samples and addition of iophenoxate to prevent fluorescence quenching by HSA during the assay was required, but otherwise no prior manipulation of the blood was required (Hatch et al. 2001). With this diffusion immunoassay Yager et al. demonstrated a limit of detection of 0.43 nM for phenytoin, and a dynamic range of three orders of magnitude (Hatch et al. 2001). The authors noted the potential of such a system for high-throughput protein substrate or drug molecule screening (Hatch et al. 2001). More recently, microfluidic technologies have been used for antibody affinity profiling of SARS-CoV-2 antibodies in human plasma (Schneider et al. 2022) and in kinetic analysis for four clinical stage anti-A β drug candidates to treat Alzheimer’s disease by using unique fingerprints to differentiate the mechanisms of action of anti-A β antibodies (Bocharov et al. 2021).

Detecting protein–protein interactions

While several microfluidic methods are being developed for detecting protein–protein interactions (e.g., (Moorthy et al. 2007; Choi et al. 2012; Salimi-Moosavi et al. 2012; Berry et al. 2014) this review focuses on those which make use of the diffusion-based measurement technique described above. As for the immunoassay developed by Yager et al. detecting protein–protein interactions using this technique relies on the principle that a complex diffuses slower than the individual components of the complex. This effect will be less pronounced in the case of interaction between two relatively large proteins than for a small molecule binding an antibody (Hatch et al. 2004). Knowles et al. recently took advantage of this technique to characterize a clinically relevant immune complex. Using their microfluidic platform to measure the hydrodynamic radii of a nanobody- α -synuclein complex, they were able to deduce that α -synuclein exists as a monomer when it binds to the single domain antibody NbSyn1—a finding that has important implications in understanding mechanisms involved in Parkinson’s disease (Yates et al. 2015). Further work in the Knowles group has seen the development of an automated high-throughput ex situ microfluidic platform for real-time tracking of amyloid formation that does not require the presence of marker molecules in the reaction mixture, opening up the possibility for a non-invasive real-time study of protein aggregation (Saar

et al. 2016). The Knowles group have also presented a mathematical approach for deconvoluting a fluorescence signal to provide a size distribution of individual components in a polydisperse sample, enabling sizing and interactions to be detected under native-like conditions (Arosio et al. 2016). Microfluidics systems have been developed to study and quantify protein–protein interactions, applications of these methodologies and microfluidic tools have been discussed in detail (Scheidt et al. 2019; Arter et al. 2020; Erkamp et al. 2022).

Observing molecular chemotaxis

The Sengupta group have used an equivalent microfluidic device to the T-sensor to demonstrate that the diffusion coefficients of both catalase and urease enzymes increase in a substrate-concentration-dependent fashion, suggesting a type of chemotactic response of enzymes towards their substrates (Sengupta et al. 2013). As no increase in diffusivity was observed for inactive enzymes, this response is attributed to catalytic activity (Sengupta et al. 2013). While the mechanism is as yet unclear, (Sengupta et al. 2013) emphasize that, in contrast to organismal chemotaxis, which requires temporal memory, enzymatic chemotaxis is postulated to be a stochastic process, which might involve nonreciprocal conformational changes. Catalase and urease both catalyze reactions that generate gas molecules (O_2 and CO_2 , respectively) which could distort fluid flow such that diffusivity of the enzyme molecules is affected. However, control experiments were carried out in which quantum dots, free fluorescent dye, or fluorescently labeled inactive enzyme were introduced into the active (unlabeled) enzyme stream, and showed that the diffusivity of these molecules did not significantly increase in the presence and absence of substrate in the adjacent buffer stream (Sengupta et al. 2013). Furthermore, a chemotactic response has also been observed for T4 DNA polymerase in response to a nucleotide triphosphate gradient (Sengupta et al. 2014), following on from similar observations by Schwartz et al. of T7 RNA polymerase (Yu et al. 2009). Sen et al. have additionally demonstrated the potential to separate active enzyme from inactive enzyme by virtue of this chemotactic response, in a microfluidic device containing multiple outlets (Dey et al. 2014). Enzymatic chemotaxis is a puzzling phenomenon that has emerged in recent years. The mechanism of enzymatic chemotaxis remains uncertain and could have implications in biotechnology and biological systems. Recent work by Feng and Gilson (Feng and Gilson 2019, 2020) critically discusses enzymatic chemotaxis and explores in detail potential mechanisms. However, they conclude elucidation of the underlying mechanism will require analysis of direct tracking studies (Sun et al. 2017; Feng and Gilson 2019, 2020)

and non-equilibrium systems with ranging scales (Feng and Gilson 2020).

Microfluidic techniques offer a conceptually simple method for the analysis of biomolecular interactions in native solution conditions relevant to their biological function compared to other methods. In recent years, microfluidic technologies for biomolecular interaction analysis, Taylor Dispersion Analysis (TDA), and Microfluidic Diffusional Sizing (MDS), have become commercially available and are represented in both technological and application literature. Continuing efforts to refine the architecture and chemistry of microfluidic devices may allow for significant increase in performance and sensitivity to interactions suggesting that microfluidic devices could have notable contribution to the future of protein–protein interaction research.

Acknowledgements RCJD acknowledges the following for funding support, in part: (1) the New Zealand Royal Society Marsden Fund (contract UOC1506); (2) a Ministry of Business, Innovation and Employment (MBIE) Smart Ideas Grant (contract UOCX1706); and (3) the Biomolecular Interaction Centre (University of Canterbury). VMN acknowledges funding provided by a MBIE Smart Ideas Grant (contract UOCX1706). SAJW acknowledges Callaghan Innovation Ltd for PhD scholarship support.

Data availability The data underlying this review are available in the review or will be shared on reasonable request to the corresponding author.

Declarations

Conflict of interest None.

References

- Arosio P, Müller T, Rajah L et al (2016) Microfluidic diffusion analysis of the sizes and interactions of proteins under native solution conditions. *ACS Nano* 10:333–341. <https://doi.org/10.1021/acsnano.5b04713>
- Arter WE, Levin A, Krainer G, Knowles TPJ (2020) Microfluidic approaches for the analysis of protein–protein interactions in solution. *Biophysical Rev* 12:575–585. <https://doi.org/10.1007/s12551-020-00679-4>
- Barbieri L, Luchinat E, Banci L (2015) Protein interaction patterns in different cellular environments are revealed by in-cell NMR. *Sci Rep-Uk* 5:14456. <https://doi.org/10.1038/srep14456>
- Berry SM, Chin EN, Jackson SS et al (2014) Weak protein–protein interactions revealed by immiscible filtration assisted by surface tension. *Anal Biochem* 447:133–140. <https://doi.org/10.1016/j.ab.2013.10.038>
- Bocharov EV, Gremer L, Urban AS et al (2021) All-d-enantiomeric peptide D3 designed for Alzheimer’s disease treatment dynamically interacts with membrane-bound amyloid- β precursors. *J Med Chem* 64:16464–16479. <https://doi.org/10.1021/acs.jmedchem.1c00632>
- Bon CL, Nicolai T, Kuil ME, Hollander JG (1999) Self-diffusion and cooperative diffusion of globular proteins in solution. *J Phys Chem B* 103:10294–10299. <https://doi.org/10.1021/jp991345a>

- Brody JP, Yager P, Goldstein RE, Austin RH (1996) Biotechnology at low Reynolds numbers. *Biophys J* 71:3430–3441. [https://doi.org/10.1016/s0006-3495\(96\)79538-3](https://doi.org/10.1016/s0006-3495(96)79538-3)
- Brody JP, Kamholz AE, Yager P (1997) Prominent microscopic effects in microfabricated fluidic analysis systems. *Micro- Nanofabricated Electro-Optical Mech Syst Biomed Environ Appl*. <https://doi.org/10.1117/12.269960>
- Brückner A, Polge C, Lentze N et al (2009) Yeast two-hybrid, a powerful tool for systems biology. *Int J Mol Sci* 10:2763–2788. <https://doi.org/10.3390/ijms10062763>
- Chaturvedi SK, Zhao H, Schuck P (2017) Sedimentation of reversibly interacting macromolecules with changes in fluorescence quantum yield. *Biophys J* 112:1374–1382. <https://doi.org/10.1016/j.bpj.2017.02.020>
- Cheng CI, Chang Y-P, Chu Y-H (2011) Biomolecular interactions and tools for their recognition: focus on the quartz crystal microbalance and its diverse surface chemistries and applications. *Chem Soc Rev* 41:1947–1971. <https://doi.org/10.1039/c1cs15168a>
- Choi J-W, Kang D-K, Park H et al (2012) High-throughput analysis of protein-protein interactions in picoliter-volume droplets using fluorescence polarization. *Anal Chem* 84:3849–3854. <https://doi.org/10.1021/ac300414g>
- Chou RY-T, Pollastrini J, Dillon TM et al (2011) Field-flow fractionation for assessing biomolecular interactions in solution. In: Williams SKR, Caldwell KD (eds) *Field-flow fractionation in biopolymer analysis*. pp 113–126
- Coglitore D, Edwardson SP, Macko P et al (2017) Transition from fractional to classical Stokes-Einstein behaviour in simple fluids. *Roy Soc Open Sci* 4:170507. <https://doi.org/10.1098/rsos.170507>
- Cole JL, Lary JW, Moody TP, Laue TM (2008) Analytical ultracentrifugation: sedimentation velocity and sedimentation equilibrium. Elsevier, Amsterdam, pp 143–179
- Collas P (2010) The current state of chromatin immunoprecipitation. *Mol Biotechnol* 45:87–100. <https://doi.org/10.1007/s12033-009-9239-8>
- Concepcion J, Witte K, Wartchow C et al (2009) Label-free detection of biomolecular interactions using bilayer interferometry for kinetic characterization. *Comb Chem High T Scr* 12:791–800. <https://doi.org/10.2174/138620709789104915>
- Costin CD, Synovec RE (2002) Measuring the transverse concentration gradient between adjacent laminar flows in a microfluidic device by a laser-based refractive index gradient detector. *Talanta* 58:551–560. [https://doi.org/10.1016/s0039-9140\(02\)00321-1](https://doi.org/10.1016/s0039-9140(02)00321-1)
- Crank J (1975) *The mathematics of diffusion*, 2nd edn. Clarendon Press,
- Creighton TE (2010) *The physical and chemical basis of molecular biology*. Helvetian Press
- Currie MJ, Manjunath L, Horne CR et al (2021) N-acetylmannosamine-6-phosphate 2-epimerase uses a novel substrate-assisted mechanism to catalyze amino sugar epimerization. *J Biol Chem* 297:101113. <https://doi.org/10.1016/j.jbc.2021.101113>
- Davies JS, Currie MJ, Wright JD et al (2021) Selective nutrient transport in bacteria: multicomponent transporter systems reign supreme. *Front Mol Biosci* 8:699222. <https://doi.org/10.3389/fmolb.2021.699222>
- Davies JS, Currie MJ, North RA et al (2022) Structure and mechanism of the tripartite ATP-independent periplasmic (TRAP) transporter. *BioRxiv*. <https://doi.org/10.1101/2022.02.13.480285>
- Demeule B, Shire SJ, Liu J (2009) A therapeutic antibody and its antigen form different complexes in serum than in phosphate-buffered saline: a study by analytical ultracentrifugation. *Anal Biochem* 388:279–287. <https://doi.org/10.1016/j.ab.2009.03.012>
- Dey KK, Das S, Poyton MF et al (2014) Chemotactic separation of enzymes. *ACS Nano* 8:11941–11949. <https://doi.org/10.1021/nl504418u>
- Dinant C, van Royen ME, Vermeulen W, Houtsmuller AB (2008) Fluorescence resonance energy transfer of GFP and YFP by spectral imaging and quantitative acceptor photobleaching. *J Microsc-Oxford* 231:97–104. <https://doi.org/10.1111/j.1365-2818.2008.02020.x>
- Einstein A (1956) *Investigations on the theory of the brownian movement*. Dover, New York
- Erkamp NA, Qi R, Welsh TJ, Knowles TPJ (2022) Microfluidics for multiscale studies of biomolecular condensates. *Lab Chip*. <https://doi.org/10.1039/d2lc00622g>
- Feng M, Gilson MK (2019) A thermodynamic limit on the role of self-propulsion in enhanced enzyme diffusion. *Biophys J* 116:1898–1906. <https://doi.org/10.1016/j.bpj.2019.04.005>
- Feng M, Gilson MK (2020) Enhanced diffusion and chemotaxis of enzymes. *Annu Rev Biophys* 49:1–19. <https://doi.org/10.1146/annurev-biophys-121219-081535>
- Germann MW, Turner T, Allison SA (2007) Translational diffusion constants of the amino acids: measurement by nmr and their use in modeling the transport of peptides. *J Phys Chem* 111:1452–1455. <https://doi.org/10.1021/jp068217o>
- Hatch A, Kamholz AE, Hawkins KR et al (2001) A rapid diffusion immunoassay in a T-sensor. *Nat Biotechnol* 19:461–465. <https://doi.org/10.1038/88135>
- Hatch A, Garcia E, Yager P (2004) Diffusion-based analysis of molecular interactions in microfluidic devices. *P IEEE* 92:126–139. <https://doi.org/10.1109/jproc.2003.820547>
- Hellman LM, Fried MG (2007) Electrophoretic mobility shift assay (EMSA) for detecting protein–nucleic acid interactions. *Nat Protoc* 2:1849–1861. <https://doi.org/10.1038/nprot.2007.249>
- Hill JJ, Laue TM (2015) Chapter twenty-one protein assembly in serum and the differences from assembly in buffer. *Methods Enzymol* 562:501–527. <https://doi.org/10.1016/bs.mie.2015.06.012>
- Horne CR, Venugopal H, Panjikar S et al (2021) Mechanism of NanR gene repression and allosteric induction of bacterial sialic acid metabolism. *Nat Commun* 12:1988. <https://doi.org/10.1038/s41467-021-22253-6>
- Ismagilov RF, Stroock AD, Kenis PJA et al (2000) Experimental and theoretical scaling laws for transverse diffusive broadening in two-phase laminar flows in microchannels. *Appl Phys Lett* 76:2376–2378. <https://doi.org/10.1063/1.126351>
- Kamholz AE, Yager P (2001) Theoretical analysis of molecular diffusion in pressure-driven laminar flow in microfluidic channels. *Biophys J* 80:155–160. [https://doi.org/10.1016/s0006-3495\(01\)76003-1](https://doi.org/10.1016/s0006-3495(01)76003-1)
- Kamholz AE, Yager P (2002) Molecular diffusive scaling laws in pressure-driven microfluidic channels: deviation from one-dimensional Einstein approximations. *Sens Actuat B Chem* 82:117–121. [https://doi.org/10.1016/s0925-4005\(01\)00990-x](https://doi.org/10.1016/s0925-4005(01)00990-x)
- Kamholz AE, Weigl BH, Finlayson BA, Yager P (1999) Quantitative analysis of molecular interaction in a microfluidic channel: the T-sensor. *Anal Chem* 71:5340–5347. <https://doi.org/10.1021/ac990504j>
- Kamholz AE, Schilling EA, Yager P (2001) Optical Measurement of transverse molecular diffusion in a microchannel. *Biophys J* 80:1967–1972. [https://doi.org/10.1016/s0006-3495\(01\)76166-8](https://doi.org/10.1016/s0006-3495(01)76166-8)
- Keene JD, Komisarow JM, Friedersdorf MB (2006) RIP-Chip: the isolation and identification of mRNAs, microRNAs and protein components of ribonucleoprotein complexes from cell extracts. *Nat Protoc* 1:302–307. <https://doi.org/10.1038/nprot.2006.47>
- Kingsbury JS, Laue TM (2011) Chapter ten fluorescence-detected sedimentation in dilute and highly concentrated solutions. *Methods Enzymol* 492:283–304. <https://doi.org/10.1016/b978-0-12-381268-1.00021-5>
- Kingsbury JS, Laue TM, Chase SF, Connors LH (2012) Detection of high-molecular-weight amyloid serum protein complexes using

- biological on-line tracer sedimentation. *Anal Biochem* 425:151–156. <https://doi.org/10.1016/j.ab.2012.03.016>
- Krayukhina E, Noda M, Ishii K et al (2017) Analytical ultracentrifugation with fluorescence detection system reveals differences in complex formation between recombinant human TNF and different biological TNF antagonists in various environments. *Mabs* 9:664–679. <https://doi.org/10.1080/19420862.2017.1297909>
- Kroe RR, Laue TM (2009) NUTS and BOLTS: applications of fluorescence-detected sedimentation. *Anal Biochem* 390:1–13. <https://doi.org/10.1016/j.ab.2008.11.033>
- Ladbury JE, Chowdhry BZ (1996) Sensing the heat: the application of isothermal titration calorimetry to thermodynamic studies of biomolecular interactions. *Chem Biol* 3:791–801. [https://doi.org/10.1016/s1074-5521\(96\)90063-0](https://doi.org/10.1016/s1074-5521(96)90063-0)
- Li Z (2009) Critical particle size where the Stokes-Einstein relation breaks down. *Phys Rev E* 80:061204. <https://doi.org/10.1103/physreve.80.061204>
- Li D, Zhang Y, He Y et al (2017) Protein-protein interaction analysis in crude bacterial lysates using combinational method of 19F site-specific incorporation and 19F NMR. *Protein Cell* 8:149–154. <https://doi.org/10.1007/s13238-016-0336-8>
- Lin MF, Larive CK (1995) Detection of insulin aggregates with pulsed-field gradient nuclear magnetic resonance spectroscopy. *Anal Biochem* 229:214–220. <https://doi.org/10.1006/abio.1995.1405>
- Linder PW, Nassimbeni LR, Polson A, Rodgers AL (1976) The diffusion coefficient of sucrose in water: a physical chemistry experiment. *J Chem Educ* 53:330. <https://doi.org/10.1021/ed053p330>
- MacGregor IK, Anderson AL, Laue TM (2004) Fluorescence detection for the XLI analytical ultracentrifuge. *Biophys Chem* 108:165–185. <https://doi.org/10.1016/j.bpc.2003.10.018>
- Mehn D, Capomaccio R, Gioria S et al (2020) Analytical ultracentrifugation for measuring drug distribution of doxorubicin loaded liposomes in human serum. *J Nanopart Res* 22:158. <https://doi.org/10.1007/s11051-020-04843-5>
- Moorthy J, Burgess R, Yethiraj A, Beebe D (2007) Microfluidic based platform for characterization of protein interactions in hydrogel nanoenvironments. *Anal Chem* 79:5322–5327. <https://doi.org/10.1021/ac070226l>
- Ouwerkerk PBF, Meijer AH (2001) Yeast one-hybrid screening for DNA-protein interactions. *Curr Protoc Mol Biology*. <https://doi.org/10.1002/0471142727.mb1212s55>
- Philibert J (2006) One and a half century of diffusion: fick, einstein, before and beyond. In: *Diffusion fundamentals*. pp. 6.1–6.19
- Philip M, Jamaluddin M, Sastry RV, Chandra HS (1979) Nucleosome core histone complex isolated gently and rapidly in 2 M NaCl is octameric. *Proc National Acad Sci* 76:5178–5182. <https://doi.org/10.1073/pnas.76.10.5178>
- Purslow JA, Khatiwada B, Bayro MJ, Venditti V (2020) NMR methods for structural characterization of protein-protein complexes. *Frontiers Mol Biosci* 7:9. <https://doi.org/10.3389/fmolb.2020.00009>
- Rattray DG, Foster LJ (2019) Dynamics of protein complex components. *Curr Opin Chem Biol* 48:81–85. <https://doi.org/10.1016/j.cbpa.2018.11.003>
- Royer CA, Scarlata SF (2008) Chapter 5 fluorescence approaches to quantifying biomolecular interactions. *Methods Enzymol* 450:79–106. [https://doi.org/10.1016/s0076-6879\(08\)03405-8](https://doi.org/10.1016/s0076-6879(08)03405-8)
- Saar K-L, Yates EV, Müller T et al (2016) Automated Ex situ assays of amyloid formation on a microfluidic platform. *Biophys J* 110:555–560. <https://doi.org/10.1016/j.bpj.2015.11.3523>
- Salimi-Moosavi H, Rathanaswami P, Rajendran S et al (2012) Rapid affinity measurement of protein–protein interactions in a microfluidic platform. *Anal Biochem* 426:134–141. <https://doi.org/10.1016/j.ab.2012.04.023>
- Saluja A, Fesinmeyer RM, Hogan S et al (2010) Diffusion and sedimentation interaction parameters for measuring the second virial coefficient and their utility as predictors of protein aggregation. *Biophys J* 99:2657–2665. <https://doi.org/10.1016/j.bpj.2010.08.020>
- Scheidt T, Łapińska U, Kumita JR et al (2019) Secondary nucleation and elongation occur at different sites on Alzheimer’s amyloid- β aggregates. *Sci Adv* 5:eaa03112. <https://doi.org/10.1126/sciadv.aaa03112>
- Schneider MM, Emmenegger M, Xu CK et al (2022) Microfluidic characterisation reveals broad range of SARS-CoV-2 antibody affinity in human plasma. *Life Sci Alliance* 5:e202101270. <https://doi.org/10.26508/lsa.202101270>
- Seidel SAI, Dijkman PM, Lea WA et al (2013) Microscale thermophoresis quantifies biomolecular interactions under previously challenging conditions. *Methods* 59:301–315. <https://doi.org/10.1016/j.ymeth.2012.12.005>
- SenGupta DJ, Zhang B, Kraemer B et al (1996) A three-hybrid system to detect RNA-protein interactions in vivo. *Proc National Acad Sci* 93:8496–8501. <https://doi.org/10.1073/pnas.93.16.8496>
- Sengupta S, Dey KK, Muddana HS et al (2013) Enzyme molecules as nanomotors. *J Am Chem Soc* 135:1406–1414. <https://doi.org/10.1021/ja3091615>
- Sengupta S, Spiering MM, Dey KK et al (2014) DNA polymerase as a molecular motor and pump. *ACS Nano* 8:2410–2418. <https://doi.org/10.1021/nn405963x>
- Shah NB, Duncan TM (2014) Bio-layer interferometry for measuring kinetics of protein-protein interactions and allosteric ligand effects. *J vis Exp*. <https://doi.org/10.3791/51383>
- Smith GP, Petrenko VA (1997) Phage display. *Chem Rev* 97:391–410. <https://doi.org/10.1021/cr960065d>
- Solovyova A, Schuck P, Costenaro L, Ebel C (2001) Non-ideality by sedimentation velocity of halophilic malate dehydrogenase in complex solvents. *Biophys J* 81:1868–1880. [https://doi.org/10.1016/s0006-3495\(01\)75838-9](https://doi.org/10.1016/s0006-3495(01)75838-9)
- Squire PG, Moser P, O’Konski CT (1968) Hydrodynamic properties of bovine serum albumin monomer and dimer. *Biochemistry-U S* 7:4261–4272. <https://doi.org/10.1021/bi00852a018>
- Squires TM, Quake SR (2005) Microfluidics: fluid physics at the nanoliter scale. *Rev Mod Phys* 77:977–1026. <https://doi.org/10.1103/revmodphys.77.977>
- Stafford WF, Szent-Gyorgyi AG (1978) Physical characterization of myosin light chains. *Biochemistry-U S* 17:607–614. <https://doi.org/10.1021/bi00597a008>
- Sun L, Gao Y, Xu Y et al (2017) Real-time imaging of single-molecule enzyme cascade using a DNA origami raft. *J Am Chem Soc* 139:17525–17532. <https://doi.org/10.1021/jacs.7b09323>
- Uchiyama S, Arisaka F, Stafford WF, Laue T (2016) Analytical ultracentrifugation. Springer, Berlin
- Weigl BH, Yager P (1997) Silicon-microfabricated diffusion-based optical chemical sensor. *Sens Actuat B Chem* 39:452–457. [https://doi.org/10.1016/s0925-4005\(96\)02120-x](https://doi.org/10.1016/s0925-4005(96)02120-x)
- Weigl BH, Yager P (1999) Microfluidic diffusion-based separation and detection. *Science* 283:346–347. <https://doi.org/10.1126/science.283.5400.346>
- Weigl BH, Holl MR, Schutte D et al. (1996) Diffusion-based optical chemical detection in silicon flow structures. *Analyt Methods Inst μ TAS 96 special edition*
- Weigl BH, Kriebel J, Mayes KJ et al (1999) Whole blood diagnostics in standard gravity and microgravity by use of microfluidic structures (T-sensors). *Microchim Acta* 131:75–83. <https://doi.org/10.1007/s006040050011>
- Wilson WD (2002) Analyzing biomolecular interactions. *Science* 295:2103–2105. <https://doi.org/10.1126/science.295.5562.2103>
- Wood DM, Dobson RCJ, Horne CR (2021) Using cryo-EM to uncover mechanisms of bacterial transcriptional regulation. *Biochem Soc T* 49:2711–2726. <https://doi.org/10.1042/bst20210674>
- Wright RT, Hayes D, Sherwood PJ et al (2018a) AUC measurements of diffusion coefficients of monoclonal antibodies in the presence

- of human serum proteins. *Eur Biophys J* 47:709–722. <https://doi.org/10.1007/s00249-018-1319-x>
- Wright RT, Hayes DB, Stafford WF et al (2018b) Characterization of therapeutic antibodies in the presence of human serum proteins by AU-FDS analytical ultracentrifugation. *Anal Biochem* 550:72–83. <https://doi.org/10.1016/j.ab.2018.04.002>
- Yager P (2003) Transverse diffusion in microfluidic systems. In: Oosterbroek RE, Berg A van den (eds) *Lab-on-a-Chip*. pp 115–150
- Yates EV, Müller T, Rajah L et al (2015) Latent analysis of unmodified biomolecules and their complexes in solution with attomole detection sensitivity. *Nat Chem* 7:802–809. <https://doi.org/10.1038/nchem.2344>
- Yu H, Jo K, Kounovsky KL et al (2009) Molecular propulsion: chemical sensing and chemotaxis of DNA driven by RNA polymerase. *J Am Chem Soc* 131:5722–5723. <https://doi.org/10.1021/ja900372m>
- Zhao H, Lomash S, Glasser C et al (2013) Analysis of high affinity self-association by fluorescence optical sedimentation velocity analytical ultracentrifugation of labeled proteins: opportunities and limitations. *PLoS ONE* 8:e83439. <https://doi.org/10.1371/journal.pone.0083439>
- Zhao H, Mayer ML, Schuck P (2014) Analysis of protein interactions with picomolar binding affinity by fluorescence-detected sedimentation velocity. *Anal Chem* 86:3181–3187. <https://doi.org/10.1021/ac500093m>

Publisher's Note Springer Nature remains neutral with regard to jurisdictional claims in published maps and institutional affiliations.

Springer Nature or its licensor (e.g. a society or other partner) holds exclusive rights to this article under a publishing agreement with the author(s) or other rightsholder(s); author self-archiving of the accepted manuscript version of this article is solely governed by the terms of such publishing agreement and applicable law.